

Influence of the Particle Size and Particle Size Ratio on the Morphology and Viscoelastic Properties of Bimodal Hard/Soft Latex Blends

Didier Colombini,[†] Helen Hassander, Ola J. Karlsson, and Frans H. J. Maurer*

Department of Polymer Science & Engineering, Lund University, Lund Institute of Technology, Box 124, SE-22100 Lund, Sweden

Received August 29, 2003

ABSTRACT: The morphology and viscoelastic properties of films prepared from bimodal latex blends containing equal weight fractions of soft and hard latex particles were investigated as a function of the particle sizes and the particle size ratio (soft particle diameter/hard particle diameter). Minimum film formation temperature (MFT) measurements were associated with transmission electron microscopy (TEM) to emphasize the particle size ratio dependence of the film formation properties. A significant increase of the MFT values with the soft/hard particle size ratio was observed. As long as the particle size ratio was low, TEM micrographs showed that the film forming soft particles, undergoing complete coalescence, clearly act as the continuous phase where the non film forming hard particles are found evenly dispersed while keeping their initial spherical shape. At higher values of the particle size ratio, TEM micrographs pointed out that the soft particles are prevented from coming into contact with each other by the surrounding hard particles, therefore dramatically increasing the MFT of the sample and resulting in a non film forming latex blend. The existence of a critical volume fraction of hard particles that is directly related to the soft/hard particle size ratio was then established on the basis of geometrical arguments involving the percolation theory. The higher the particle size ratio, the lower the critical volume fraction of hard particles that leads to a macroscopic phase inversion resulting in a non film forming bimodal latex blend. Subsequently, the mechanical film properties were investigated by solid-state dynamic mechanical analysis. The size of the dispersed hard phase was found to affect the final viscoelastic film properties. The smaller the size of the hard particles, the better the mechanical enhancement of the mechanical film properties. Last, the experimental viscoelastic thermograms were compared with some theoretical predictions based on self-consistent mechanical modeling. The final film properties of the bimodal hard/soft latex blends were then directly connected to the film formation properties.

1. Introduction

The technology involving polymer blends has been a major area of research in the past decades. Most classes of polymer blends have been discussed^{1–5} in great detail, including engineering polymer blends, polyolefin blends, reactive blends, and glassy polymer/elastomer blends. The one area of polymer blends that has been virtually ignored involves simple latex blends. Recently, an increasing number of publications have appeared^{6–40} that investigate the characteristics of film formation and the mechanical film properties of blends of polymer dispersions.

An area of specific scientific and technical interest involves the combination of hard and soft latexes. Basically, it is expected that a dispersion of latex with a glass transition temperature (T_g) below room temperature (i.e., soft latex) will form a continuous film upon evaporation at room temperature even when blended with a substantial amount of high- T_g latex (i.e., hard latex). Although the presence of aggregates of hard particles could affect the transparency of latex blend films, the addition of hard latex particles was reported^{13–15,39} as greatly improving the mechanical performance of latex blends. When compared to that of the soft polymer, the dynamic storage modulus of the

hard/soft latex blends was significantly increased and stayed decently high at elevated temperatures, i.e., far above the T_g of the soft polymer. In addition, it was also established³⁹ that transparent latex blend films require that the hard latex particles be sufficiently small and well dispersed in the final film.

With a similar challenging intention of developing room-temperature film forming latexes which exhibit improved mechanical properties, Eckersley and Helmer¹² reported that the addition of hard latex particles in a soft film forming latex significantly improved the block resistance of the resulting hard/soft latex blend films. Although it was concluded¹² that the hard phase could be viewed as an inert filler, it was also pointed out that hard/soft latex blends showed highly desirable final properties, provided that their soft/hard particle size ratio was large. It was also mentioned that a careful control of the particle sizes, particle size ratio and hard/soft blend composition is required when one wants to produce hard/soft latex blends with desired film formation properties.

There are numerous fundamental parameters (including physical, chemical, geometrical, and environmental parameters) that govern the complex relationship between the film formation, the morphology, and the final film properties of latex blends. The aim of the present paper was to investigate the influence of the particle sizes and the particle size ratio on the morphology and viscoelastic film properties of bimodal hard/soft

* Corresponding author. E-mail: frans.maurer@polymer.lth.se. Telephone: +46 46222 91 49. Fax +46 46 22 41 15.

[†] Present address: Fibre Science and Communication Network, Mid Sweden University, SE-851 70 Sundsvall, Sweden.

Table 1. Chemicals and Recipes for the Latex Preparation

chemicals (<i>suppliers</i>)		latex recipes (wt %)			
		large soft (LgSf)	small soft (SmSf)	large hard (LgHd)	small hard (SmHd)
initial charge of the reactor	demineralized water	32.27	31.85	31.91	31.52
	sodium dodecyl sulfate (<i>BDH Lab. Suppl.</i>)	0.01	0.21	0.01	0.21
	sodium carbonate (<i>BDH Lab. Suppl.</i>)	0.02	0.02	0.02	0.02
	pre-emulsion (part of the feed, see below)	50 mL			
initiator	sodium persulfate (<i>Aldrich</i>)	5 mL + 2 × 1 mL of a solution of 4.0 g of Na ₂ S ₂ O ₈ in 10 mL of demineralized water			
pre-emulsion feed to the reactor	demineralized water	29.19	28.85	28.82	28.50
	sodium dodecyl sulfate (<i>BDH Lab. Suppl.</i>)	0.33	1.29	0.33	1.28
	sodium carbonate (<i>BDH Lab. Suppl.</i>)	0.03	0.03	0.03	0.03
	methyl methacrylate (<i>Aldrich</i>)	17.18	17.00	35.00	34.60
	butyl acrylate (<i>Aldrich</i>)	20.97	20.75		
	styrene (<i>Aldrich</i>)			3.88	3.84
Σ (wt %)		100.00	100.00	100.00	100.00

Table 2. Composition of the Bimodal Hard/Soft Latex Blends

systems		composition (wt %)				latex blends: sample codes
		LgSf	SmSf	LgHd	SmHd	
bimodal binary	50	0	0	50	100	LgSf50/SmHd50
	50	0	50	0	100	LgSf50/LgHd50
	0	50	0	50	100	SmSf50/SmHd50
	0	50	50	0	100	SmSf50/LgHd50
bimodal multiple	25	25	0	50	100	LgSf25/SmSf25/SmHd50
	30	20	0	50	100	LgSf30/SmSf20/SmHd50
	40	10	0	50	100	LgSf40/SmSf10/SmHd50
	0	50	25	25	100	SmSf50/LgHd25/SmHd25
	0	50	10	40	100	SmSf50/LgHd10/SmHd40
	25	25	50	0	100	LgSf25/SmSf25/LgHd50
	25	25	25	25	100	LgSf25/SmSf25/LgHd25/SmHd25

latex blends in connection with the film formation properties.

2. Sample Preparation and Characterization

2.1. Materials and Latex Preparation. 2.1.1. Materials. All chemicals and suppliers involved in the neat latex recipes are given in Table 1. The monomers, i.e., styrene (Sty), methyl methacrylate (MMA), and butyl acrylate (BuA), were first purified by passing them through a column filled with aluminum oxide (Aldrich, active base), and then they were kept at 5 °C before use. All other chemicals were of analytical grade and used as supplied.

2.1.2. Latex Preparation. The three fundamental parameters of particular relevance to the present work are the particle size, the particle size ratio, and the glass transition temperature of the neat latexes. Thus, four separate neat latex dispersions were synthesized. All of the particles are based on copolymers of MMA, and either BuA or Sty. The recipes, which are given in detail in Table 1, were defined by taking into account the Fox law⁴¹ with the intention to reach T_g values either lower (typically ≤ 5 °C) or higher (≥ 110 °C) than room temperature. In Table 1, these neat latexes are referred to either as soft (Sf) when $T_g <$ room temperature or as hard (Hd) when $T_g >$ room temperature. They were prepared through semibatch emulsion polymerization in a 2000 mL reactor (ChemiSens, RM-2L)^{42,43} using sodium dodecyl sulfate (SDS) as the emulsifier and sodium persulfate as the initiator. By properly adjusting the amount of SDS, it was also possible to control the particle size of the dispersions, that is referred to in Table 1 as small (Sm) or large (Lg).

As described in Table 1, demineralized water, SDS, and sodium carbonate were initially charged into the reactor together with a certain amount of a pre-emulsion that consists of monomers and all the other chemicals except the initiator. Under gentle mechanical stirring, the reactor content was repeatedly degassed and purged with nitrogen before it was heated to the polymerization temperature (i.e., 65 °C) and held there for 30 min. Adding the initiator solution then started

the reaction. Subsequently, the reactor was continuously fed (under mechanical stirring) with the rest of the pre-emulsion for about 3 h, using a variable-speed motor-driven syringe, which was also repeatedly degassed and purged with nitrogen prior to the beginning of the feed. The reactor was then held at 65 °C for 1 h under stirring and, finally, slowly cooled to room temperature.

2.2. Latex Blends. Film Preparation. Bimodal hard/soft latex blends were prepared by mixing (using a magnetic stirrer) equivalent weights of hard and soft latex dispersions in order to always keep a final hard/soft blend ratio equal to 1. After 10 min of mixing, 4 g of the mixture of dispersions was cast into Petri dishes with similar surface areas (~ 40 cm²) and allowed to dry under the ambient conditions of the laboratory. The final dried latex film thickness achieved by this method was approximately 400 μ m.

Although the bimodal blend compositions were all equal to 50/50 (Hd/Sf wt %), the investigated bimodal latex blends (presented in Table 2) were divided into two series, referred to as binary or as multiple systems, depending on how many neat dispersions were involved in the hard and soft phases. Basically, the bimodal binary hard/soft systems corresponded to latex blends whose hard and soft phases involved two neat dispersions (i.e., one each), whereas the bimodal multiple systems involved more than two neat dispersions (i.e., more than one for at least one of the phases).

In the present paper, the latex blends are denoted with a view to describing their composition in weight percent of each neat latex dispersion (see Table 2). For example, the sample code LgSf25/SmSf25/LgHd25/SmHd25 corresponds to a bimodal multiple hard/soft latex blend based on 25 wt % of each of the neat dispersions described in Table 1.

2.3. Sample Characterization. 2.3.1. Solids Content. The solids content of the neat latex dispersions was measured gravimetrically. Approximately 3 g of the dispersions was poured into test tubes and was allowed to dry overnight in an oven at 60 °C. The data reported in the paper correspond to the average from a set of 5 measurements.

2.3.2. Particle Size. Quasielastic Light Scattering (QELS). Quasielastic light scattering (QELS) measurements were performed using a Coulter model N4MD particle sizer. Prior to the measurements, the neat latexes were diluted with doubly distilled, deionized, and doubly filtered (Millipore, 100 nm) water in order to minimize the influence of dust particles. The measurements were carried out at room temperature at a scattering angle of 90°. The reported results are averages of 20 runs having a dust factor of 0%.

2.3.3. Density. A Quantachrome Corporation Ultrapycometer-1000 (using nitrogen gas) was used to determine the density of the neat latex films. Samples of ~1 g were placed in the measurement cell at a controlled temperature of 26 °C. Prior to the measurements, an equilibrium time of 20 min was selected. All the density values given here correspond to the average of five measurements with a maximum standard deviation of 0.05%.

2.3.4. Minimum Film Formation Temperature (MFT). The minimum film formation temperature (MFT) was measured on a thermostair MFT gradient bridge (Coesfeld, GmbH, Germany) having a controlled temperature interval ranging either from -3 to +35 °C or from 30 to 60 °C in a static atmosphere, using freshly regenerated silica gel applied on a grid in the MFT bridge to obtain a controlled environment with no airflow and constant relative humidity. The dispersion samples that consisted of neat latexes and bimodal latex blends were applied with an applicator bar with a gap thickness of 200 μ m on a metal foil. The MFT was defined as the crack-point temperature above which the dispersion would form a continuous film.

2.3.5. Differential Scanning Calorimetry (DSC). The differential scanning calorimetry (DSC) thermograms were recorded using a TA Instruments DSC-Q1000 under N₂ atmosphere. The samples were first jumped from room temperature to 150 °C, maintained at 150 °C for 3 min, and then cooled at 10 °C/min down to -70 °C. After 3 min equilibrium time at -70 °C, the samples were heated to 180 °C with a heating rate of 10 °C/min. The weight of the samples was about 5 mg.

2.3.6. Dynamic Mechanical Analysis (DMA). The TA Instruments "dynamic mechanical analyzer" DMA 2980 was used, operating in tensile mode under isochronal conditions at the frequency of 1 Hz, to measure the temperature dependence of the absolute value of the complex elastic modulus $|E^*|$ (storage, E' , and loss, E'' , moduli) and loss factor $\tan \delta$ of the films. The viscoelastic spectra were recorded from -110 to +200 °C with a heating rate of 2 °C/min. The samples were approximately 12 mm long, 5 mm wide, and 400 μ m thick.

2.3.7. Transmission Electron Microscopy (TEM). The samples were examined in a Philips CM 10 transmission electron microscope. To investigate their film formation properties, each 50/50 bimodal hard/soft mixture was first diluted to 0.1 wt % solids. A drop of the latex was then placed on a Formvar-coated grid and the excess water was removed by adsorbing with a filter paper. Micrographs were recorded on negative films, which were subsequently scanned.

In the micrographs, the PS phase appeared as dark and the MMA-co-BuA phase as bright domains.⁴⁴

2.4. Theoretical Considerations. Self-Consistent Schemes. The dynamic mechanical properties of multiphase polymeric materials, such as polymer blends, can be theoretically investigated by mechanical modeling either based on phenomenological laws⁴⁵⁻⁴⁷ and variational methods,⁴⁸⁻⁵⁰ or based on self-consistent schemes,⁵¹⁻⁵⁷ for which the static elastic solutions are extended to the viscoelastic ones through the correspondence principle.⁵⁸ When compared to the others, mechanical models based on self-consistent schemes do not require any adjustable parameters to perform the numerical calculations.

The self-consistent interlayer model^{54,59} used in this work has been well presented⁵⁹⁻⁶¹ and requires the definition of a representative volume element (RVE) in order to predict the dynamic mechanical shear properties of multipolymeric materials having a particulate morphology. An RVE, as typically involved in the numerical simulations, consists of three

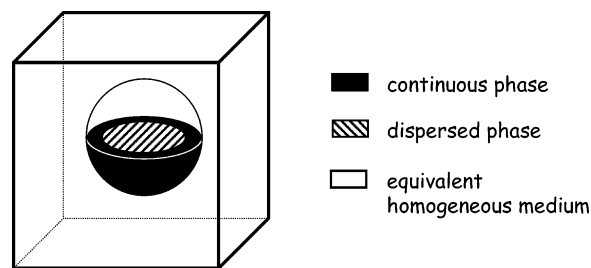


Figure 1. Illustration of a representative volume element (RVE) of the interlayer model.

concentric spheres embedded in an equivalent homogeneous medium. This geometrical arrangement not only is representative of the "particle-interphase-matrix" morphology of a three-phase particulate system but also takes into account the composition of the multicomponent material through the radii of the concentric spheres. Basically, such an RVE, that is independent of the dispersed particle size, is therefore expected to respond to external stresses, as would do the homogeneous blend material. From a theoretical point of view, it is possible to perform numerical simulations by assuming a volume fraction of interphase equal to zero, therefore leading to the prediction of the viscoelastic properties of a two-phase particulate system. An illustration of the corresponding two-phase RVE is given in Figure 1.

In the present work, two distinct geometrical arrangements have been used for the numerical calculations. Both involve a two-phase particulate morphology (as depicted in Figure 1) where the soft latex either acts as the continuous or as the dispersed phase, and simultaneously vice versa for the hard latex.

3. Results and Discussion

3.1. Properties of Dispersions and Films of the Neat Latexes. The neat latexes (LgSf, SmSf, LgHd, and SmHd) were all characterized before blending. The soft neat latexes were film-forming under the ambient conditions of the laboratory (both LgSf and SmSf having an MFT value around 0 °C), whereas the hard ones could not form a film (MFT > 60 °C) and became white powders when left overnight for drying. To be able to characterize them by DMA, a certain amount of each of these SmHd and LgHd powders was placed in a mold between two aluminum foils and heat-pressed at 180 °C for 8 min, followed by 2 min under 10 tons of pressure. Following this procedure, clear hard films with a thickness of around 500 μ m were obtained.

The main characteristics of the four neat latexes are reported in Table 3. In the wet state, equivalent solids contents (~39 wt %) were observed for all the dispersions, and the sizes of the particles were found to decrease with increasing amount of SDS (i.e., surfactant) in the latex recipes (Table 1). In addition, it can be noticed that the size ratio between large and small particles was roughly equal to 4, similarly for the two soft latexes (ratio = 336/86) and for the two hard ones (ratio = 237/54).

In the dry state, the densities of the two soft films were found to be (Table 3) similar to each other but slightly higher than those of the hard films, whose densities were also close to each other. Also reported in Table 3 are the T_g values of the four neat latexes. The T_g 's of the soft systems were similar and lower than 5 °C, and those of the hard latexes were both found to be slightly higher than 110 °C. The investigated bimodal latex blends (presented in Table 2) therefore all displayed a constant $\Delta T_g \sim 110$ °C between their hard and

Table 3. Properties of the Neat Latexes

		neat latexes			
	properties	LgSf	SmSf	LgHd	SmHd
dispersions (wet stage)	solids content (wt %)	38.9	38.8	38.2	39.1
	particle size (nm)	336	86	237	54
films (dried stage)	density at 26°C (g·cm ⁻³)	1.119	1.121	1.061	1.069
	<i>T</i> _g (°C) ^a	2 ± 1	3 ± 1	114 ± 1	118 ± 1

^a Obtained by DSC at the inflection point of the change in the baseline.

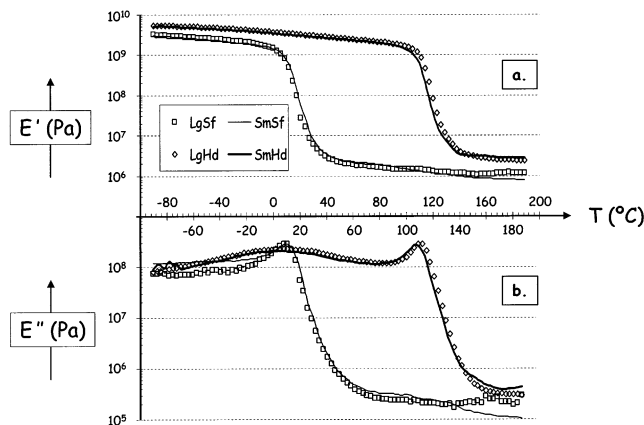


Figure 2. Viscoelastic properties (at 1 Hz) of the neat latex films. (a) Storage modulus (E') vs temperature. (b) Loss modulus (E'') vs temperature.

soft constituents, independent of their respective phase composition.

The mechanical viscoelastic properties of the neat latexes are given in Figure 2. It can be noticed that the α -relaxations, associated with the glass transition, of the soft films were located in the same temperature range. Both led to a significant drop of the storage modulus (between -20 and $+60$ °C in Figure 2a) coupled with a maximum of the loss modulus (Figure 2b) located at (10.5 ± 0.5) °C for the LgSf film and at (11.0 ± 0.5) °C for the SmSf film. In agreement with earlier observations,¹² such a superimposition in the mechanical spectra (E' and E'') of both LgSf and SmSf films points out that the particle size does not influence the viscoelastic properties of the neat soft constituents.

Similarly, the maxima of E'' (Figure 2b) following the drop of E' (between 90 and 160 °C in Figure 2a) observed for the LgHd and SmHd films were also found close to each other, and located at (109.5 ± 0.5) °C and at (112.5 ± 0.5) °C, respectively.

In summary, all the bimodal hard/soft latex blends that were investigated in this paper were based on the mixing of one or two hard neat dispersions with one or two soft ones. One would have to keep in mind that the investigated bimodal latex blends only differed by the size of the particles and the resulting soft/hard particle size ratio, whereas many other experimental parameters (such as the blend composition, the solids contents of the dispersions, the densities of the soft films and those of the hard ones, T_g^{soft} , T_g^{hard} , and ΔT_g) were identical for all the presented systems. Such bimodal systems can therefore be viewed as suitable models for studying the influence of both the particle size and the soft/hard particle size ratio on the film formation and mechanical film properties of latex blends.

3.2. Film Formation Properties of the Bimodal Latex Blends. **3.2.1. Particle Size and Particle Size Ratio.** Taking into account the composition of the bimodal blends of dispersions (Table 2), and all the

particle sizes, densities, and solids contents of the neat latexes (Table 3), it was possible to estimate the number (N_k) of latex particles that were from each of the neat latex dispersions (k) involved in 1 g of each bimodal blend, as follows:

$$N_k = \frac{S_k w_k}{d_k} \cdot \frac{1}{4\pi D_k^3} \quad (\text{I})$$

where k is related to LgSf, SmSf, LgHd, or SmHd (all dispersions considered as monodisperse), with S_k , d_k , and D_k referring to the solids content [wt %], to the density [g·cm⁻³] and to the latex particle size [cm] of the neat latex k , respectively, and w_k is the weight fraction [wt %] of the dispersion k that was introduced in the bimodal mixture.

Subsequently, the surface-average particle sizes of the soft and the hard particles (denoted D_{soft} and D_{hard} , respectively) can be calculated⁶² as follows:

$$D_{\text{soft}} = \frac{\sum_i N_i D_i^3}{\sum_i N_i D_i^2} \quad (\text{II})$$

where i refers either to LgSf or to SmSf and

$$D_{\text{hard}} = \frac{\sum_j N_j D_j^3}{\sum_j N_j D_j^2} \quad (\text{III})$$

where j refers either to LgHd or to SmHd.

D_{soft} and D_{hard} values obtained for the bimodal binary and multiple latex blends are all reported in Table 4, together with their corresponding particle size ratio $D_{\text{soft}}/D_{\text{hard}}$. Despite the fact that all the systems have the same 50/50 hard/soft blend composition, it can be noticed that an interesting set of values was obtained for D_{soft} and D_{hard} , leading to particle size ratios $D_{\text{soft}}/D_{\text{hard}}$ ranging from 0.36 to 6.22.

It was deemed to be of interest to study the dependence of the film formation properties on the particle sizes D_{soft} and D_{hard} and on the particle size ratio $D_{\text{soft}}/D_{\text{hard}}$.

3.2.2. Minimum Film Formation Temperature.

An important characteristic related to the film formation properties of latexes is the minimum film formation temperature (MFT). MFT determination is commonly performed in the coatings industry and considered as the primary indicator of the lower temperature range over which a latex can be used in applications.^{22,25,35,40} Below this critical temperature, the dry latex is opaque and powdery. Several definitions of MFT were reported in the literature.^{7,11,22,25,35,40,63} As mentioned in the Experimental Section, MFT has been considered in the

Table 4. Surface-Average Particle Sizes and Particle Size Ratios and MFT's of the Latex Blends

systems	latex blends: sample codes	surface-average particle sizes (D_{soft} and D_{hard}) and particle size ratios			MFT's (°C)
		D_{soft} (nm)	D_{hard} (nm)	$D_{\text{soft}}/D_{\text{hard}}$	
bimodal binary	LgSf50/SmHd50	336	54	6.22	40 ± 2
	LgSf50/LgHd50	336	237	1.42	7 ± 2
	SmSf50/SmHd50	86	54	1.59	8 ± 2
	SmSf50/LgHd50	86	237	0.36	5 ± 2
bimodal multiple	LgSf25/SmSf25/SmHd50	138	54	2.55	14 ± 2
	LgSf30/SmSf20/SmHd50	156	54	2.90	17 ± 2
	LgSf40/SmSf10/SmHd50	214	54	3.96	30 ± 2
	SmSf50/LgHd25/SmHd25	86	83	1.04	5 ± 2
	SmSf50/LgHd10/SmHd40	86	62	1.38	6 ± 2
	LgSf25/SmSf25/LgHd50	138	237	0.58	6 ± 2
	LgSf25/SmSf25/LgHd25/SmHd25	138	83	1.66	8 ± 2

present study as the temperature above which the cast latex dispersion formed a coherent film.

The MFT values measured for all our bimodal latex blends are reported in Table 4. It can first be noticed that the MFT values were significantly different, ranging from (5 ± 2) to (40 ± 2) °C. To study the influence of the soft particle size on the MFT, Figure 3a presents the evolution of the MFT values measured for bimodal systems having a constant D_{hard} as a function of D_{soft} . The MFT values were clearly found to be affected by the soft particle size, and had a tendency to increase linearly with D_{soft} at a constant D_{hard} . For a given set of drying conditions and constant D_{hard} , a better film formation is therefore expected for latex blends when the soft particles are smaller. As mentioned earlier,¹³ this result suggests that smaller soft particles can more efficiently fill the interstitial spaces between the hard particles. As a direct consequence, it can also be noticed in Figure 3a that the smaller the D_{hard} , the more pronounced the dependence of MFT on D_{soft} .

Similarly, Figure 3b shows the evolution of the MFT values obtained for bimodal blends with a constant D_{soft} , as a function of the hard particle size D_{hard} . Although the influence of D_{hard} on MFT was much less pronounced than that of D_{soft} , it can be observed that the MFT values decreased when D_{hard} increased. However, the D_{hard} dependence of MFT was not linear, and the MFT values were found to quickly reach a plateau corresponding to the MFT of the soft particles.

An interesting way to associate the MFT measurements of all our bimodal systems is presented in Figure 3c, where the evolution of the MFT values is given as a function of the soft/hard particle size $D_{\text{soft}}/D_{\text{hard}}$. When plotted together in such a way, it is relevant to notice that the MFT data all belong to a unique curve. Such a sigmoidal evolution of MFT following the increase of $D_{\text{soft}}/D_{\text{hard}}$ (Figure 3c) points out that the MFT values of the bimodal latex blends were strongly influenced by the soft/hard particle size ratio.

The crucial dependence of the film formation properties of the bimodal blends on the particle size ratio is clearly illustrated in Figure 4, which shows TEM micrographs recorded during the film formation of diluted (0.1 wt %) 50/50 bimodal hard/soft mixtures of various particle size ratio. The TEM pictures of the three bimodal binary latex blends, that were SmSf50/LgHd50 ($D_{\text{soft}}/D_{\text{hard}} = 0.36$), LgSf50/LgHd50 ($D_{\text{soft}}/D_{\text{hard}} = 1.42$), and LgSf50/SmHd50 ($D_{\text{soft}}/D_{\text{hard}} = 6.22$) are presented in Figure 4a to Figure 4c, respectively. Seeing as the styrene had a higher stability than the acrylics in the electron beam,⁴⁴ the styrene-rich hard phase appeared dark in the TEM micrographs, whereas the

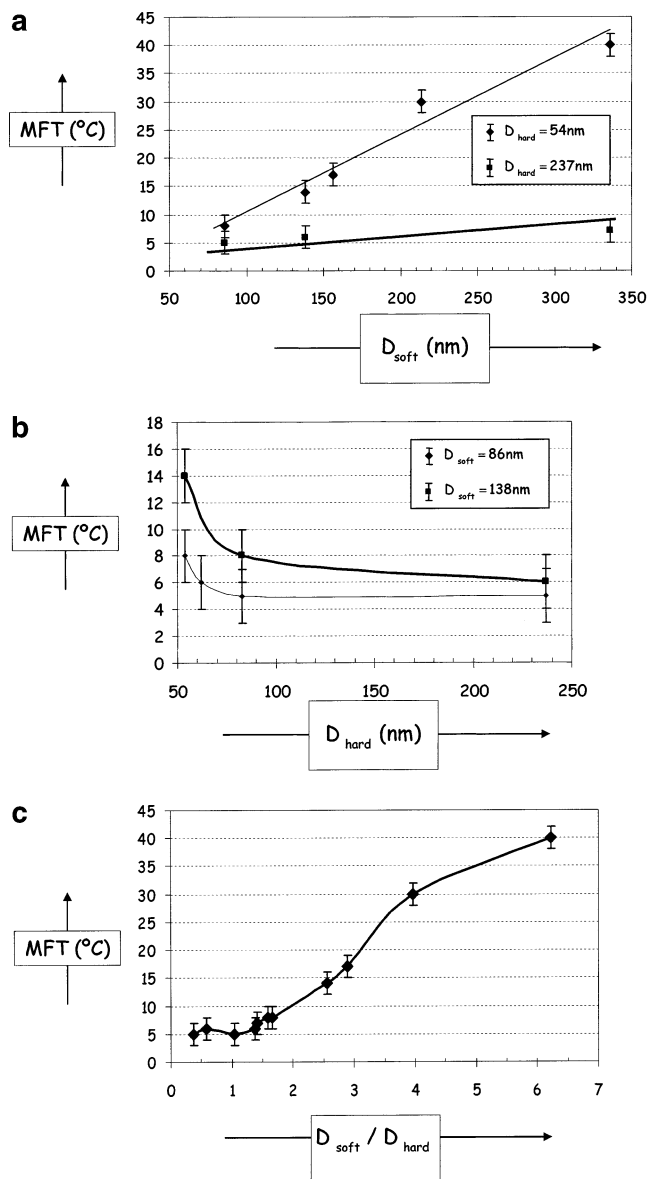


Figure 3. Minimum film formation temperature (MFT) of the latex blends as a function of (a) the particle size of the soft phase (D_{soft}), (b) the particle size of the hard phase (D_{hard}), and (c) the particle size ratio ($D_{\text{soft}}/D_{\text{hard}}$).

P(MMA-*co*-BuA) soft phase corresponded to the bright areas.

At a lower value of the particle size ratio (Figure 4a), the bimodal SmSf50/LgHd50 latex blend was film forming and the soft particles, having undergone complete coalescence, clearly acted as the continuous phase

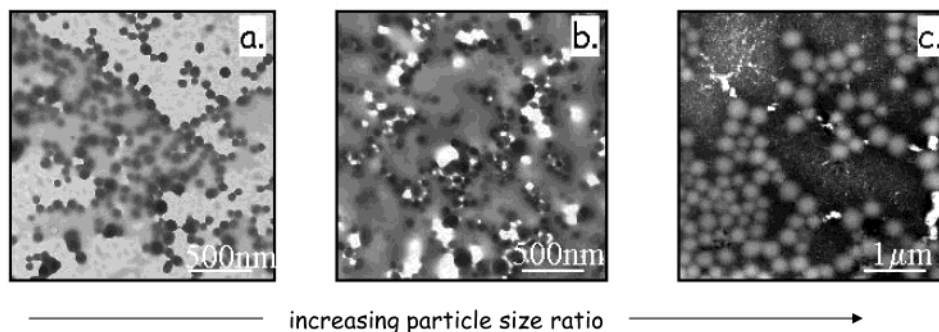


Figure 4. TEM micrographs during the film formation of bimodal latex blends with different particle size ratio: (a) SmSf50/LgHd50; (b) LgSf50/LgHd50; (c) LgSf50/SmHd50. The films were formed under the ambient conditions of the laboratory. For a clearer overview, the scale of Figure 4c differs from that of Figure 4, parts a and b.

where the dark hard particles were evenly dispersed while they kept their spherical shape. Although the LgSf50/LgHd50 blend remained film forming, the hard particles were shown to be less well dispersed in the soft matrix where a nonnegligible fraction of voids (see white domains in Figure 4b) was also observed. At a higher particle size ratio (Figure 4c), the soft particles were found slightly deformed from their original spherical shape but prevented to come into contact with each other in order for them to coalesce by the surrounding spherical hard particles. An inversion of the continuous phase was therefore observed (Figure 4c), and the presence of cracks can be noticed within the dark phase in the TEM micrograph of the resulting nonfilm forming LgSf50/SmHd50 latex blend.

The particle size ratio is therefore here presented as a parameter of primary importance for better understanding and control of the film formation properties of bimodal latex blends, independent of both the latex blend composition and the neat latex properties. The results of our investigation fully support earlier observations^{8–10,12–16,20,22,25,30,31,35,36,39,40} and discussions.^{12,13,36} As a matter of fact, the particle size ratio was for example found¹² to have a dramatic effect on the block resistance of bimodal poly(styrene-*co*-butyl acrylate) latex blends: the best performance was observed for the highest value of $D_{\text{soft}}/D_{\text{hard}}$. Other papers focusing on the film transparency^{13,36} pointed out that, for a given latex blend composition, transparent films were easily achieved when the particle size ratio was low. When put together, it comes out that these observations^{8–10,12–16,20,22,25,30,31,35,36,40} were actually mainly dependent on the ability or nonability of the hard particles to come into contact with each other and to form a continuous percolated network during the film formation of the latex blends. The idea of taking into account the percolation concept⁶⁴ in latex blends was initially proposed by Eckersley and Helmer,¹² who have made use of the concept of phase continuity (initially developed⁶⁵ for the study of the dispersion of fine metallic powders into polymeric systems) to suggest that optimal particle packing could be achieved in their blends depending on the particle size ratio. In bimodal latex blends, when one aims to enhance the final mechanical film properties, the idea is to reach final film morphologies where the hard particles are finely dispersed within a soft continuous matrix. As long as the volume fraction of the hard phase does not exceed a critical value leading to the percolation of the nonfilm forming particles, the bimodal latex blends remain film forming. Above this critical volume fraction of hard particles, the soft particles cannot prevent the percola-

tion of the hard ones, which leads, during the drying process, to a macroscopic phase inversion that dramatically shifts the MFT of the bimodal blend toward the higher temperatures. On the basis of the geometrical arguments involving the percolation theory proposed by Eckersley and Helmer,¹² it becomes clear from the results presented in Figure 3c and Figure 4, that such a critical value is directly related to the particle size ratio. The higher the particle size ratio $D_{\text{soft}}/D_{\text{hard}}$, the lower the critical volume fraction of hard particles leading to percolation. Before starting the preparation of latex blend series over a whole blend composition range, our present investigation would therefore first recommend to have a look on the particle size ratio of the studied systems, then to quickly estimate^{12,36} the critical volume fraction of hard particles that is related to this $D_{\text{soft}}/D_{\text{hard}}$ ratio.

The next section will be devoted to the mechanical film properties of the bimodal latex blends. Especially, the influences of both the dispersed particle size and the particle size ratio on the final film properties will be discussed.

3.3. Film Properties of the Latex Blends. 3.3.1. Influence of the Dispersed Particle Size. To study the influence of D_{hard} on the final mechanical film properties, two series of bimodal latex blends have been investigated by DMA. Within a series, the soft phase of the selected blends was always kept identical. Subsequently, the MFT values of blends that belong to the same series were also similar.

Thus, the first series involved the three bimodal blends SmSf50/LgHd50, SmSf50/LgHd25/SmHd25, and SmSf50/LgHd10/SmHd40: these blends all had similar MFT's ($\sim 5^\circ\text{C}$, see Table 4) as well as an identical soft phase based on SmSf50 ($D_{\text{soft}} = 86\text{ nm}$, Table 3). Therefore, they differed only in the size of their dispersed hard particles, ranging from 237 to 62 nm (Table 4), respectively. Similarly, two latex blends, with soft phase based on LgSf25/SmSf25 and with similar MFT's ($\sim 7^\circ\text{C}$, see Table 4) were chosen for the second blend series.

The temperature dependence of the dynamic storage modulus recorded for these two series are presented in parts a and b of Figure 5, respectively. The viscoelastic properties of the neat latexes involved in the series are also recalled in Figure 5 for comparison.

Similar observations can be drawn from the thermomechanical spectra of the two series of bimodal blends. First of all, it can be noticed that all the latex blends showed two distinct transitions, to which drops in E' values corresponding to the α -relaxation of both the soft

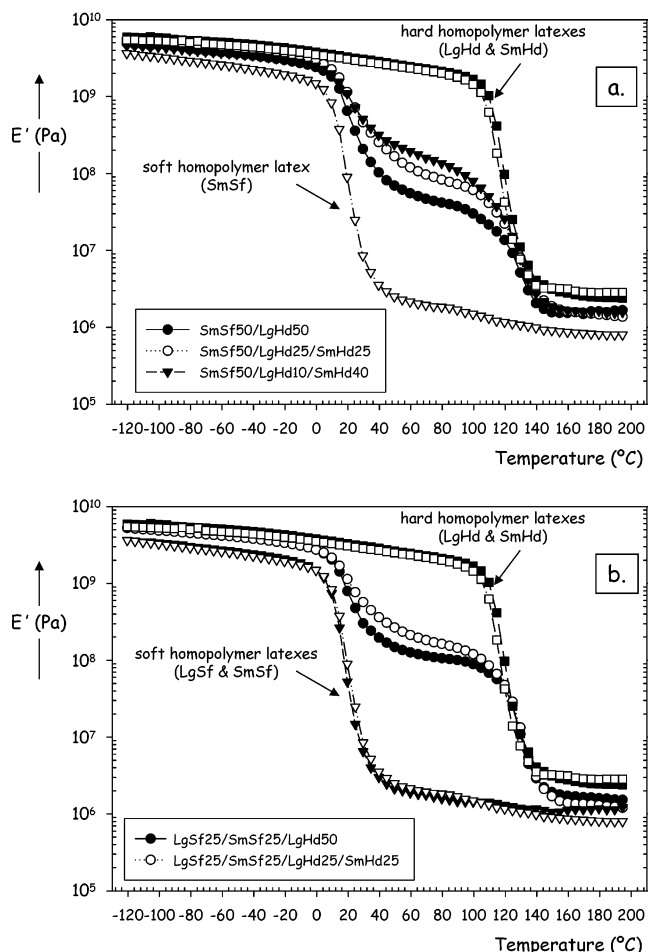


Figure 5. Influence of the dispersed particle size on the viscoelastic properties of the latex blends: (a) blends based on SmSf50 as matrix; (b) blends based on LgSf25/SmSf25 as matrix. The viscoelastic behavior of the neat latex films is recalled for comparison.

and the hard phases in the blends were associated. Such viscoelastic spectra are typical of films with phase separated morphologies.^{1,2,53,58,66} In addition, the temperature location of the drops in E' values for the blends were found rather close to those separately recorded for both soft and hard neat latexes.

The main feature pointed out in Figure 5 is the significant enhancement of the mechanical film properties that can be noticed at temperatures between the α -relaxations of both the soft and the hard phases, where the storage modulus of the latex blends was found far above that of the neat soft constituent. In addition, it can be observed that the mechanical enhancement of the blends was found (Figure 5, parts a and b) to be more pronounced when the size of the dispersed hard particles decreased, whatever the soft phase. This is a strong indication that these bimodal systems can all be considered as phase separated blends with morphology involving a soft matrix filled with hard spheres.^{1,2,12,53,58,66–68}

3.3.2. Influence of the Particle Size Ratio. As mentioned in the previous section, the size of the dispersed hard particles affected the viscoelastic film properties. Therefore, to focus on the sole influence of $D_{\text{soft}}/D_{\text{hard}}$ on the mechanical film properties, two bimodal binary latex blends, i.e., LgSf50/LgHd50 ($D_{\text{soft}}/D_{\text{hard}} \sim 1.42$) and SmSf50/LgHd50 ($D_{\text{soft}}/D_{\text{hard}} \sim 0.36$) that both had a hard phase based on LgHd50, were chosen. As a

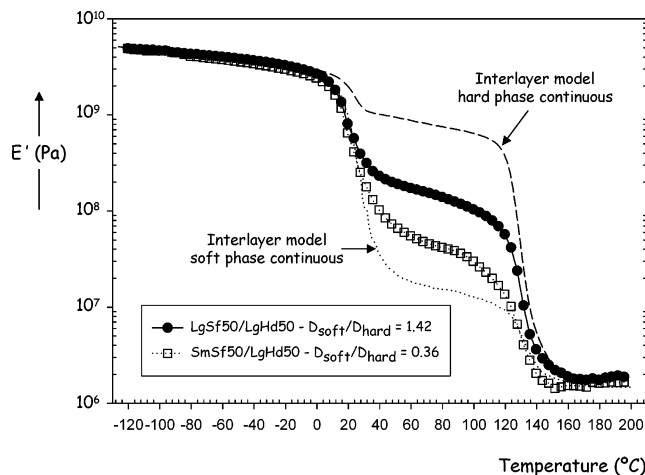


Figure 6. Influence of the particle size ratio on the viscoelastic properties of latex blends based on LgHd particles.

consequence of the difference in the particle size ratios of these two blends, the MFT value of the LgSf50/LgHd50 sample (MFT $\sim 7 \pm 2$ °C, Table 4) was slightly higher than that of the SmSf50/LgHd50 blend (MFT $\sim 5 \pm 2$ °C, Table 4), but both values remained similar.

Figure 6 shows the temperature dependence of the mechanical storage modulus of the two bimodal binary latex blends. In addition, two theoretical predictions of the viscoelastic properties of these blends are also given in Figure 6. These numerical calculations were performed using the self-consistent interlayer model^{54,59,60,66} by taking into account two distinct two-phase particulate morphologies. In the first case, the soft latex was considered as the continuous phase, in which the hard latex particles were dispersed. The second simulation involved the opposite morphology, i.e., the hard latex acted as the continuous phase.

From the experimental thermomechanical spectra (Figure 6), significant differences were found between the two latex blends, especially in the temperature range between the α -relaxations of both the soft and the hard phases. Thus, it can be noticed that the enhancement in the mechanical properties was higher for the bimodal system with the highest particle size ratio (i.e., LgSf50/LgHd50). Similar observations related to the influence of $D_{\text{soft}}/D_{\text{hard}}$ on the magnitude of the storage modulus of latex blends were mentioned earlier,¹² but they were interpreted as resulting from the decrease in the dispersed particle size. In the present study, both the hard particle size and the blend composition have been kept identical. Therefore, the differences in the experimental mechanical spectra result from the sole difference in the particle size ratio of the two bimodal latex blends.

Concerning the theoretical viscoelastic spectra, it should first be noticed that both predicted thermomechanical evolutions of the storage modulus (Figure 6) were clearly distinct, and mainly influenced by the continuous phase.^{1,58,66} When associated together with the experimental data, it comes out (Figure 6) that when $D_{\text{soft}}/D_{\text{hard}}$ decreased, the experimental viscoelastic spectra became more and more close to the theoretical evolution of E' assuming a continuous soft phase. Such an observation may be interpreted as indicating a better quality of the soft matrix in the SmSf50/LgHd50 blend, i.e., preventing the aggregation of hard particles.^{9,10} It was also found^{66,68,69} that the presence of such aggregates of particles in filled systems resulted in an

additional contribution of mechanical coupling between the phases, which, in the viscoelastic thermogram, led to a significant additional increase of the storage modulus of the filled systems. Insofar as $D_{\text{soft}}/D_{\text{hard}}$ of the LgSf50/LgHd50 blend was higher than that of SmSf50/LgHd50, the critical volume fraction of hard particles was expected to be lower (see above in section 3.2.2) in the case of LgSf50/LgHd50. Subsequently, it can be reasonably assumed that the aggregation of the LgHd particles may have at least partially taken place in the LgSf50/LgHd50 sample. Even if the entire percolation of the hard particles was not achieved (the LgSf50/LgHd50 sample being film forming), the existence of such aggregates of hard particles would therefore explain the observed differences between the experimental dynamic mechanical spectra of the two bimodal latex blends (Figure 6). Our interpretation of the higher storage modulus of the LgSf50/LgHd50 blend as resulting from the presence of aggregates of LgHd particles, whose presence can be justified by a higher particle size ratio compared to the SmSf50/LgHd50 blend, was also supported by the TEM micrographs (Figure 4, parts a and b).

4. Conclusion

The influence of both the particle size and the particle size ratio on the morphology and on the final viscoelastic film properties of bimodal 50/50 (wt %) hard/soft latex blends was investigated in connection with the resulting changes in the film formation properties.

Four different neat latex dispersions were synthesized and characterized; bimodal hard/soft latex blends were then prepared by mixing them while keeping a final hard/soft blend composition equal to 50/50. It was shown that the investigated latex blends only differed by the size of the particles and their resulting soft/hard particle size ratio.

The minimum film formation temperature (MFT) of the bimodal systems was determined. Although the influences of the soft (D_{soft}) and the hard (D_{hard}) particle sizes on MFT were also discussed, the strong influence of the particle size ratio $D_{\text{soft}}/D_{\text{hard}}$ on the MFT values was especially emphasized: thus, the MFT values were found to significantly increase with $D_{\text{soft}}/D_{\text{hard}}$.

In addition, the particle size ratio dependence of the film forming properties was also investigated by transmission electron microscopy. It was clearly observed that the hard particles acted as the dispersed phase in the blends as long as the particle size ratio was low, and in agreement with a correspondingly low MFT, the soft particles formed the continuous phase. At higher $D_{\text{soft}}/D_{\text{hard}}$, it was found that the soft particles were prevented from coming into contact with each other by the surrounding hard particles, resulting in dramatically increased MFT's of the samples and non film forming latex blends. Subsequently, it was concluded that as long as the volume fraction of the hard phase in the bimodal latex blend did not exceed a critical value leading to the percolation of the nonfilm forming particles, the bimodal latex blends remain film forming. Above this critical value, the latex blend was no longer film forming at room temperature. On the basis of geometrical arguments involving the percolation theory, such a critical volume fraction of hard particles was presented as directly related to the particle size ratio: the higher $D_{\text{soft}}/D_{\text{hard}}$, the lower the critical volume fraction of hard particles leading to percolation.

The mechanical film properties were last investigated by solid-state dynamic mechanical analysis. The size of the dispersed hard phase was found to affect the final viscoelastic film properties. The smaller the size of the hard particles, the better the mechanical enhancement of the mechanical film properties. In addition, the experimental viscoelastic data were also compared with some theoretical predictions based on self-consistent mechanical modeling. It was then established that the final film properties of such 50/50 bimodal latex blends are directly connected to the film formation properties, which are strongly influenced by the particle size ratio of the soft and hard phases.

Finally, it should be brought to the attention of the reader that the consequences of thermal annealing on the viscoelastic properties and morphologies of these 50/50 bimodal hard/soft latex blends have also been investigated and are reported in a separate paper.⁷⁰

Acknowledgment. The authors would like to thank Frida Karlsson at Celanese Emulsions Norden AB (Perstorp, Sweden) for the MFT measurements and Daniela Vidovska, LTH (Lund, Sweden) for her participation in the synthesis of the neat latexes. We also gratefully acknowledge the VINNOVA and Industry sponsored Centre for Amphiphilic Polymers from Renewable Resources (Sweden) for the financial support of this work.

References and Notes

- (1) Bohn, L. In *Copolymers, polyblends, and composites*; Platzer, N. J. J., Ed.; Advances in Chemistry 6; American Chemical Society: Washington, DC, 1974.
- (2) Lipatov, Y. S. *Physical Chemistry of filled polymers*; Rubber and Plastics Research Association of Great Britain: Shrewsbury, England, 1979.
- (3) Utracki, L. A. *Polymer alloys and blends: Thermodynamics and Rheology*; Hanser Publishers: Munich, Germany, Vienna, and New York, 1989.
- (4) Miles, I. S.; Rostami, S. *Multicomponent Polymer Systems*; Longman Scientific & Technical: Singapore, 1992.
- (5) Paul, D. R.; Newman, S. *Polymer blends*; Academic Press: London, 1978.
- (6) Agarwal, N.; Farris, R. J. *J. Appl. Polym. Sci.* **1999**, 72, 1407.
- (7) Brodnyn, J. G.; Konen, T. *J. Appl. Polym. Sci.* **1964**, 8, 687.
- (8) Cavaillé, J. Y.; Vassoile, R.; Thollet, G.; Rios, L.; Pichot, C. *Colloid Polym. Sci.* **1991**, 269, 248.
- (9) Chevalier, Y.; Hidalgo, M.; Cavaillé, J. Y.; Cabane, B. *Symposium on Latex Film formation: Proceedings*; Chicago, 1995.
- (10) Chevalier, Y.; Hidalgo, M.; Cavaillé, J.-Y.; Cabane, B. *Macromolecules* **1999**, 32, 7887.
- (11) Eckersley, S. T.; Rudin, A. *J. Coat. Technol.* **1990**, 62, 89.
- (12) Eckersley, S. T.; Helmer, B. J. *J. Coat. Technol.* **1997**, 69, 97.
- (13) Feng, J.; Winnik, M. A.; Shivers, R. R.; Clubb, B. *Macromolecules* **1995**, 28, 7671.
- (14) Feng, J.; Winnik, M. A. *Macromolecules* **1997**, 30, 4324.
- (15) Feng, J.; Odobina, E.; Winnik, M. A. *Macromolecules* **1998**, 31, 5290.
- (16) Feng, J.; Winnik, M. A.; Siemiarczuk, A. *J. Polym. Sci., Part B: Polym. Phys.* **1998**, 36, 1115.
- (17) Gauthier, C.; Perez, J. *Polym. for Adv. Technol.* **1995**, 6, 276.
- (18) Gauthier, C.; Guyot, A.; Perez, J.; Sindt, O. *Am. Chem. Soc. Symp. Ser.* **1996**, 648, 163.
- (19) Haba, Y.; Segal, E.; Narkis, M.; Titelman, G. I.; Siegmann, A. *Synth. Met.* **2000**, 110, 189.
- (20) Heuts, M. P. J.; Le Fèvre, R. A.; Van Hilst, J. L. M.; Overbeek, G. C. *Am. Chem. Soc. Symp. Ser.* **1996**, 648, 271.
- (21) Ho, C. C.; Khew, M. C.; Liew, Y. F. *Surf. Interface Anal.* **2001**, 32, 133.
- (22) Jensen, D. P.; Morgan, L. W. *J. Appl. Polym. Sci.* **1991**, 42, 2845.

- (23) Jourdan, C.; Cavaillé, J. Y.; Perez, J. *Polym. Eng. Sci.* **1988**, 28, 1318.
- (24) Keddie, J. L.; Meredith, P.; Jones, R. A. L.; Donald, A. M. *Langmuir* **1996**, 12, 3793.
- (25) Keddie, J. L. *Mater. Sci. Eng. R: Rep.* **1997**, 21, 101.
- (26) Lepizzera, S.; L'hommeau, C.; Dilger, G.; Pith, T.; Lambla, M. *J. Polym. Sci., Part B: Polym. Phys.* **1997**, 35, 2093.
- (27) Nemirovski, N.; Narkis, M. *Adv. Chem. Ser., Am. Chem. Soc.* **1994**, 239, 353.
- (28) Nemirovski, N.; Narkis, M. *Polym. Eng. Sci.* **1994**, 34, 750.
- (29) Odrobina, E.; Feng, J.; Pham, H. H.; Winnik, M. A. *Macromolecules* **2001**, 34, 6039.
- (30) Patel, A. A.; Feng, J.; Winnik, M. A.; Vancso, G. J. *Polymer* **1996**, 37, 2277.
- (31) Peters, A. C. I. A.; Overbeek, G. C.; Buckmann, A. J. P.; Padget, J. C.; Annable, T. *Prog. Org. Coat.* **1996**, 29, 183.
- (32) Robeson, L. M.; Berner, R. A. *J. Polym. Sci., Part B: Polym. Phys.* **2001**, 39, 1093.
- (33) Robeson, L. M.; Vratsanos, M. S. *Macromol. Symp.* **2000**, 155, 117.
- (34) Richard, J.; Maquet, J. *Polymer* **1992**, 33, 4164.
- (35) Steward, P. A.; Hearn, J.; Wilkinson, M. C. *Adv. Colloid Interface Sci.* **2000**, 86, 195.
- (36) Tzitzinou, A.; Keddie, J. L.; Geurts, J. M.; Peters, A. C. I. A.; Satguru, R. *Macromolecules* **2000**, 33, 2695.
- (37) Vorobyova, O.; Winnik, M. A. *Macromolecules* **2001**, 34, 2298.
- (38) Vorobyova, O.; Winnik, M. A. *J. Polym. Sci., Part B: Polym. Phys.* **2001**, 39, 2317.
- (39) Winnik, M. A.; Feng, J. R. *J. Coating Technol.* **1996**, 68, 39.
- (40) Winnik, M. A. In *Emulsion polymerization and emulsion polymers*; Lovell, P. A., El-Aasser, M. S., Ed.; John Wiley & Sons Ltd.: 1997; p 467.
- (41) Fox, T. G. *Bull. Am. Phys. Soc.* **1956**, 1.
- (42) Nilsson, H.; Silvergren, C.; Törnell, B. *Chem. Scr.* **1982**, 19, 164.
- (43) Karlsson, O. J.; Hassander, H.; Wesslen, B. *J. Appl. Polym. Sci.* **2000**, 77, 297.
- (44) Thompson, E. V. *J. Polym. Sci., Part B: Polym. Phys.* **1965**, 3, 675.
- (45) Kardos, J. L.; Raison, J.; Piccarolo, S.; Halpin, J. C. *Polym. Eng. Sci.* **1979**, 19, 1000.
- (46) Kolarik, J. *Polym. Eng. Sci.* **1996**, 36, 2518.
- (47) Takayanagi, M.; Imida, K.; Kajiyama, T. *J. Polym. Sci., Part C: Polym. Symp.* **1966**, 15, 263.
- (48) Voigt, V. *Lehrbuch der Kristallphysik*; Teuber: Berlin, 1910.
- (49) Reuss, A. *Z. Angew. Math. Mech.* **1929**, 9, 49.
- (50) Hashin, Z.; Shtrickman, S. *J. Mech. Phys. Solids* **1963**, 11, 127.
- (51) Hill, R. *J. Mech. Phys. Solids* **1965**, 13, 213.
- (52) Hervé, E.; Zaoui, A. *Int. J. Eng. Sci.* **1993**, 31, 1.
- (53) Budiansky, B. *J. Mech. Phys. Solids* **1965**, 13, 223.
- (54) Maurer, F. H. J. In *Polymer Composites*; Sedlacek, B., Ed.; W. de Gruyter & Co.: Berlin, 1986; 399.
- (55) Davies, W. E. A. *J. Phys. D: Appl. Phys.* **1971**, 4, 1325.
- (56) Davies, W. E. A. *J. Phys. D: Appl. Phys.* **1971**, 4, 1176.
- (57) Christensen, R. M.; Lo, K. H. *J. Mech. Phys. Solids* **1979**, 27, 315.
- (58) Dickie, R. A. *J. Appl. Polym. Sci.* **1973**, 17, 45.
- (59) Maurer, F. H. J. In *Controlled interphases in composite materials*; Ishida, H., Ed.; Elsevier Science Publishing Co.: New York, 1990; 491.
- (60) Eklind, H.; Maurer, F. H. J. *Polymer* **1996**, 37, 2641.
- (61) Colombini, D.; Maurer, F. H. J. *Macromolecules* **2002**, 35, 5891.
- (62) http://www.chem.usyd.edu.au/~gilbert/IUPAC_Polymer_Colloid_termnlg.pdf.
- (63) Winnik, M.; Wang, Y.; Haley, F. *J. Coat. Technol.* **1992**, 64, 51.
- (64) De Gennes, P. G. In *Scaling concept in polymer physics*; Cornell University Press: Ithaca, NY, 1979.
- (65) Kusy, R. P. *J. Appl. Phys.* **1977**, 48, 5301.
- (66) Colombini, D.; Merle, G.; Alberola, N. D. *J. Appl. Polym. Sci.* **2000**, 76, 530.
- (67) Ouali, N.; Cavaillé, J. Y.; Perez, J. *J. Plast. Rubber Compos. Process. Appl.* **1991**, 16, 55.
- (68) Colombini, D.; Merle, G.; Alberola, N. D. *Macromolecules* **2001**, 34, 5916.
- (69) Mele, P.; Alberola, N. D. *Compos. Sci. Technol.* **1996**, 56, 849.
- (70) Colombini, D.; Hassander, H.; Karlsson, O. J.; Maurer, F. H. J. Effects of thermal annealing on the viscoelastic properties and morphology of bimodal hard/soft latex blends. *J. Polym. Sci.: Polym. Phys.*, submitted 2003.

MA030455J